Analysis of the Magnetic Coupling in M-3(dpa)(4)Cl-2 Systems (M = Ni, Pd, Cu, Ag) by Ab Initio Calculations

ARTICLE *in* THE JOURNAL OF PHYSICAL CHEMISTRY A · FEBRUARY 2010

Impact Factor: 2.69 · DOI: 10.1021/jp910763d · Source: PubMed

3 AUTHORS:

Zahra Tabookht
Universitat Rovira i Virgili
6 PUBLICATIONS **26** CITATIONS
SEE PROFILE

Xavier López
Universitat Rovira i Virgili
67 PUBLICATIONS **1,600** CITATIONS
SEE PROFILE

Coen de Graaf
Universitat Rovira i Virgili
139 PUBLICATIONS **2,415** CITATIONS
SEE PROFILE

Analysis of the Magnetic Coupling in $M_3(dpa)_4Cl_2$ Systems (M = Ni, Pd, Cu, Ag) by Ab Initio Calculations

Zahra Tabookht,[†] Xavier López,*[,†] and Coen de Graaf[†,‡]

Departament de Química Física i Inorgànica, Universitat Rovira i Virgili, C/Marcel·lí Domingo s/n, 43007, Tarragona, Spain, and Institució Catalana de Recerca i Estudi Avançats (ICREA), Passeig Lluís Companys 23, 08010 barcelona, Spain

Received: November 12, 2009; Revised Manuscript Received: December 11, 2009

The magnetic exchange parameter (J) of a series of neutral and oxidized trinuclear extended metal atom chain complexes $[M_3(dpa)_4Cl_2]^{0/1+}$, where dpa is the anion of di(2-pyridyl)amine, has been extracted employing the complete active space second-order perturbation theory (CASPT2). The computed magnetic coupling constant for $Ni_3(dpa)_4Cl_2$ (-98 cm^{-1}) and the mono-oxidized Cu_3 complex (-35 cm^{-1}) are in excellent agreement with the experimental estimates. This consistence is though not achieved for $Cu_3(dpa)_4Cl_2$, with three $S = 1/2$ magnetic centers, for which we surprisingly obtain 1/3 of the experimental value only. This worrying result and the possible sources for such large discrepancy are analyzed. The magnetic coupling has been also analyzed for the hypothetical complexes with Pd_3 and Ag_3 metal chains. Much larger couplings are obtained, which is ascribed to the larger spatial extent of the magnetic orbitals. Furthermore, we analyze the relative importance of the magnetic coupling paths through the σ-system (through metal coupling) and the δ-system (through ligand coupling).

Introduction

In the past 30 years, much experimental, theoretical, and computational effort has been devoted to the understanding, rationalization, and prediction of magnetic properties of all kinds of known and hypothetical systems.[1] Among molecular magnetic systems, multinuclear metal complexes have attracted much attention due to their diverse applications in nanoscale electronic devices[2] and their peculiar spin interactions. Since molecule-based magnets usually contain transition metal (TM) atoms and a large number of ligands, the computational approaches handled to reach satisfactory results may lie at the equilibrium point between accuracy and computational time. Whereas for the computation of optical electronic transitions an accuracy of 0.2 eV ($\approx$1600 cm^{-1}) is considered a good result, for magnetic observables this is far from being acceptable. Notwithstanding, the calculation of the relative energies of the electronic states involved in magnetic properties is feasible due to the fact that the states have the same electronic configuration and geometry, reducing the possible sources of inaccuracies. Experience shows that a precision of 10$-$50 cm^{-1} is not unusual.

Trimetallic complexes are the simplest prototypical examples of extended metal atom chains (EMACs) that have been extensively studied due to their appealing magnetic and conducting properties.[3] The structure of a trimetallic complex with formula $M_3(dpa)_4Cl_2$ is shown in Figure 1 where a linear string of three transition metals is surrounded helically by four organic ligands. The family of the dipyridylamido ligands is employed for this purpose. The chain is capped at both ends by two chloride ions. EMAC complexes with a different number and type of metal atoms have been synthesized and structurally characterized principally by the groups of Peng[4] and Cotton.[5]

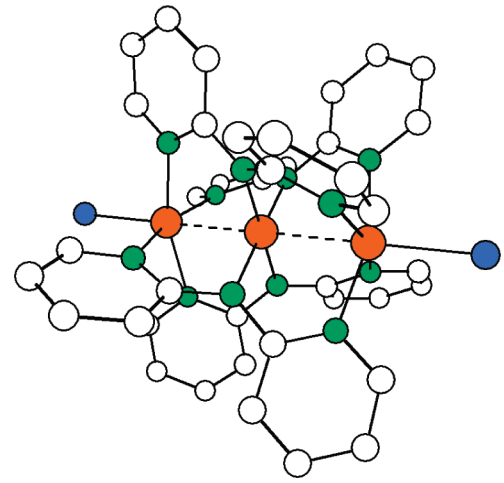

Figure 1. Ball-and-stick representation of trimetallic EMACs. Color coding for atoms: orange, metals; green, nitrogen; blue, chlorine; white, carbon. Hydrogens are not represented for clarity.

The metal$-$metal interactions have been interesting for understanding electron transport through the linear metal chains as well.[6]

Theoretical studies on EMAC systems have been exclusively performed to date with density functional theory (DFT) schemes, mainly due to their relatively large size.[3e−m] These theoretical works have provided deeper insight into the electronic structure and the magnetic coupling in these systems. In general, qualitatively correct estimates of exchange coupling constants have been obtained. The main problem of DFT in describing magnetic couplings, that is, the impossibility to introduce static correlation in some electronic states, motivated the present work. We herein employ a multiconfigurational (MC) approach, which properly accounts for the static electron correlation and describes all spin states as eigenstates of the total spin operator.

* Corresponding author. E-mail: javier.lopez@urv.cat.
[†] Universitat Rovira i Virgili.
[‡] Institució Catalana de Recerca i Estudi Avançats (ICREA).

10.1021/jp910763d
Published on Web 01/06/2010

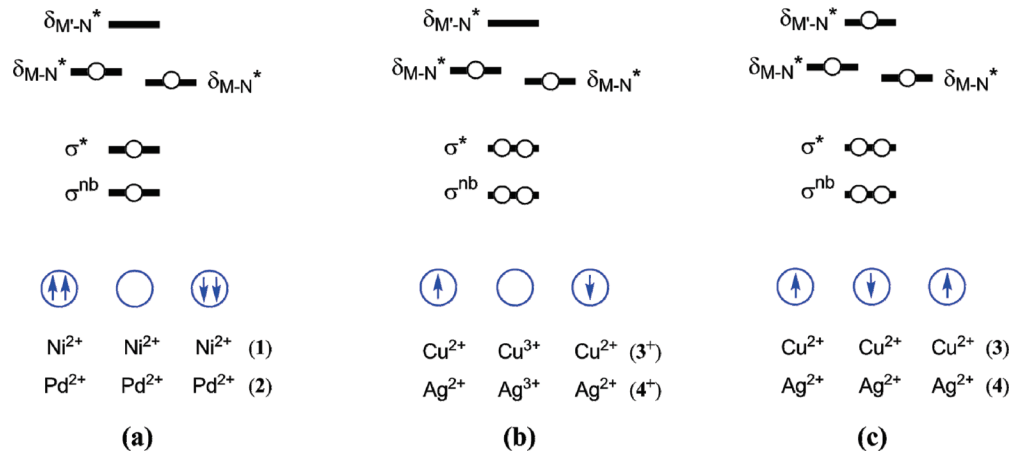

Figure 2. Schematic view of the electron distribution involved in the magnetic coupling in (a) **1** and **2**, (b) $\mathbf{3}^+$ and $\mathbf{4}^+$, and (c) **3** and **4** EMAC string complexes. The molecular orbitals shown are the upper five of the set of 15 containing the metal valence electrons. The energy separation between the orbitals represented is not scaled.

TABLE 1: Selected Interatomic Distances (Å) Computed at the DFT/B3LYP Level for $Ni_3(dpa)_4Cl_2$ (1), $Pd_3(dpa)_4Cl_2$ (2), $Cu_3(dpa)_4Cl_2$ (3), $[Cu_3(dpa)_4Cl_2]^+$ ($\mathbf{3}^+$), $Ag_3(dpa)_4Cl_2$ (4), and $[Ag_3(dpa)_4Cl_2]^+$ ($\mathbf{4}^+$) in Their Ground States[a]

	1	**2**	**3**	$\mathbf{3}^+$	**4**	$\mathbf{4}^+$
M−M	2.481 (2.42−2.44)	2.544	2.531 (2.47−2.49)	2.571 (2.51)	2.695	2.695
M−Cl	2.399 (2.33−2.34)	2.564	2.498 (2.44−2.49)	2.470 (2.39)	2.639	2.627
$M-N_{term}$	2.125 (2.08−2.10)	2.258	2.116 (2.06−2.09)	2.084 (2.06)	2.323	2.266
$M-N_{cent}$	1.922 (1.88−1.89)	2.062	2.004 (1.96−1.98)	1.922 (1.89)	2.184	2.093

[a] The experimental distances of **1**, **3**, and $\mathbf{3}^+$, in parentheses, are taken from ref 3a, c, and d, respectively.

The complete active space self-consistent field (CASSCF) method is, in principle, a good technique to this aim, but the dimension of the active space mainly limits its applicability. However, in most problems related to magnetism, the number of electrons and orbitals that have to be included in the CAS remains below this limit, and good results can be obtained by combining CASSCF with a second computational technique to account for the dynamical electron correlation, such as the complete active space second-order perturbation theory (CASPT2)[7] or the difference dedicated configuration interaction (DDCI).[8] A second drawback of this approach is the number of basis functions that can be treated in a straightforward routine-like fashion. Until recently, the CASSCF+CASPT2/DDCI method has mostly been applied to relatively small molecules, but the development of new formulations based on the Cholesky decomposition of the integrals[9] and/or local electron correlation methods[10] significantly extended the region of applicability of these MC approaches. Since highly correlated treatments of TM complexes with magnetic interactions have been devoted only to modestly large complexes,[11] this work explores the possibilities of applying such methods to large molecules. Here, we analyze the exchange coupling constants obtained for a series of EMAC complexes using the CASPT2 methodology.[12] This method uses a CAS wave function as zeroth-order wave function and accounts for the remaining part of the electron correlation with second-order perturbation theory. Normally, CASPT2 gives rather satisfactory results provided that the CAS is large enough and properly chosen.[13] This latter issue is important in the discussion of the results.

The ab initio data herein presented for $Ni_3(dpa)_4Cl_2$ (**1**), $Pd_3(dpa)_4Cl_2$ (**2**), $Cu_3(dpa)_4Cl_2$ (**3**), $Cu_3(dpa)_4Cl_2^+$ ($\mathbf{3}^+$), $Ag_3(dpa)_4Cl_2$ (**4**), and $Ag_3(dpa)_4Cl_2^+$ ($\mathbf{4}^+$) are discussed and compared to those computed before at the DFT level. The presentation of the results is organized in two main parts: first the string complexes containing two magnetic centers (**1**, **2** and $\mathbf{3}^+$, $\mathbf{4}^+$) and then the compounds with three magnetic centers (**3**, **4**). A schematic representation of the electronic structure of the compounds discussed in the present article is shown in Figure 2.

Computational Details

The geometries of all the structures studied were optimized with the Gaussian03 implementation[14] of the density functional theory (DFT) using the hybrid B3LYP exchange-correlation functional. This level of calculation, applied to EMACs by Bénard and colleagues during the past decade, has proven useful in their geometrical and electronic characterizations and also in the rationalization of such metal chains' magnetic properties.[3e−m,4n,r,s,6c] Double-ξ valence basis sets have been used for light atoms (H, C, N). Los Alamos electron−core potentials were used for Cl and metal atoms, and double-ξ functions for valence electrons (LANL2DZ basis sets). Polarization functions have been added for nitrogen (d) and metal atoms (f) to get more accurate and reliable geometries since small geometrical distortions can have an important impact in the study of magnetic interaction problems. The geometry optimizations have been carried out for $Ni_3(dpa)_4Cl_2$, $Cu_3(dpa)_4Cl_2$, and $Ag_3(dpa)_4Cl_2$ in their corresponding ground states using the unrestricted formalism. We used the ground state optimized geometries for $Pd_3(dpa)_4Cl_2$, $[Cu_3(dpa)_4Cl_2]^+$, and $[Ag_3(dpa)_4Cl_2]^+$ as previously published.[3l,g] The main structural parameters of the optimized geometries are displayed in Table 1. For the three complexes that have been synthesized to date, namely **1**, **3**, and $\mathbf{3}^+$, the calculated interatomic distances compare well with the experimental ones, although being slightly longer in general. This is a well-known default of most functionals.

All CASSCF/CASPT2 calculations were carried out with the MOLCAS 7 suite of programs.[15] Atomic natural orbitals of ANO-RCC type were employed as the basis set for all atoms.[16] For Ni and Cu atoms, we employed (5s,4p,3d) basis sets, for

Ag and Pd atoms (6s,5p,4d), for the bridging N atoms (3s,2p), and for axial Cl ligands (4s,3p). Also, C and H atoms were assigned (3s,2p) and (2s) basis sets, respectively. One prerequisite for working with MOLCAS is decreasing the full symmetry point group of the molecule to the largest symmetry subgroup that does not contain degenerate irreducible representations. For this reason, the original full symmetry has been reduced from D_4 to D_2, and the molecular orbitals in this new symmetry belong to a, b_1, b_2, and b_3 symmetries.

In all CASPT2 calculations, a low reference weight (RW = 0.29) has been observed. Low RWs can be caused either by the presence of undesired intruder states or by the large number of correlated electrons. To fix this shortcut, removal of the intruder states is performed introducing a level shift to the CASPT2 calculation. The present calculations always give RWs ~0.29−0.30 for level shifts ranging from 0.0 to 0.2, indicating that the intruder states are not the cause of such low RWs, but the large amount of correlated electrons. The criteria which guarantee the reliability and accuracy of the calculations are the energy differences between different states as long as they are calculated with an as similar as possible active space in CASSCF calculations and with the similar reference weights in CASPT2 calculations.

For a molecule with only two magnetic centers, the Heisenberg Hamiltonian, which is the summation over all the nearest spin-carrying neighboring interactions,[17] takes this simple form

$$\hat{H} = -J\hat{S}_1\hat{S}_2$$

where J is the exchange coupling constant, and S_1 and S_2 are the spin moments localized on each magnetic center. Since EMACs are antiferromagnetic in nature, the following discussions are based on the fact that the ground state is an open-shell singlet. For two $S = 1/2$ magnetic centers, the two possible eigenfunctions (the ground state singlet and the triplet) have associated energies $(3/4)J$ and $-(1/4)J$, respectively. In this case, J is exactly the energy gap between states. When each interacting center bears a maximal $S = 1$ spin moment, a quintet state also appears in addition to the triplet and singlet coupled state. The eigenvalue of the singlet ground state is equal to $2J$, and for the excited triplet and the quintet the eigenvalues are J and $-J$, respectively.

The energy spectrum normally follows the so-called Landé pattern predicted by the Heisenberg Hamiltonian: $E(S - 1) - E(S) = SJ$. Deviations may however be observed when the number of energy levels increases due to the existence of elevated spin moments on the TM centers. In these cases, the Heisenberg Hamiltonian can be extended with extra terms such as the isotropic biquadratic exchange or anisotropy (zero-field splitting) terms. It was recently found that the intrinsic precision of CASPT2 does not allow studying the deviations to the Heisenberg Hamiltonian.[18] Therefore, we will report CASPT2 estimates of J as average of the slightly different J-values that can be extracted from the full spectrum.

For linear systems with three magnetic centers, the spin Hamiltonian describing the low-lying states is defined as

$$\hat{H} = -J_1(\hat{S}_1\hat{S}_2 + \hat{S}_2\hat{S}_3) - J_2\hat{S}_1\hat{S}_3$$

in which J_1 and J_2 represent the exchange parameter between nearest neighbors and next-nearest neighbors, respectively. The eigenfunctions of this Hamiltonian for $S = 1/2$ magnetic centers are two doublet states and one quartet state with energies

$$\text{Doublets: } E(1/2,\text{A}) = J_1 - (1/4)J_2;\ E(1/2,\text{B}) = (3/4)J_2$$

$$\text{Quartet: } E(3/2) = -(1/2)J_1 - (1/4)J_2$$

Thus, the quartet excited state is separated in energy by $-(3/2)J_1$ from the doublet ground state. The interaction between next-nearest neighbors (J_2) in molecules with three magnetic centers is much weaker than that between neighboring metals (J_1), as we will show in the Results section. The last term in the Heisenberg Hamiltonian can then be ignored without altering the main conclusions of the study.

Results and Discussion

1. Molecules with Two Magnetic Centers. *$Ni_3(dpa)_4Cl_2$* (1) *and $Pd_3(dpa)_4Cl_2$* (2). These systems are characterized by featuring four unpaired electrons located in four molecular orbitals, namely, σ^*, σ^{nb}, and two $\delta_{M(terminal)-N}^*$. These orbitals have major contributions from the terminal metal atoms, and hence, the magnetic interaction occurs between electrons localized at both ends of the string (see Figure 2). In contrast, the central metal presents a diamagnetic configuration induced by the four amino groups to which it is coordinated. In these complexes with two $S = 1$ centers, the magnetic coupling takes place by two main mechanisms. The first one originates in the electrons occupying σ orbitals. The second one is a consequence of an indirect coupling of the δ electrons involving the bridging ligand orbitals and the x^2-y^2 orbital of the central metal which lies at the crossing point of four equivalent magnetic interaction pathways.[3h] The part of the magnetic coupling associated to the σ interaction is the leading interaction as it takes place through the central Ni atom only and by a very effective overlap of d_z^2 orbitals. In $Ni_3(dpa)_4Cl_2$, the interaction between the two outermost Ni(II) atoms is antiferromagnetic, with experimental J lying between -99 and -108 cm^{-1} (Peng's group[4a] and Cotton's group[3a] data, respectively). The Pd homologue, **2**, has not been reported experimentally, but a DFT study was recently performed.[3l]

To describe the magnetic behavior of **1** and **2** with ab initio methods, we first construct a wave function in the minimal active space with the orbitals involved in the magnetic interaction (Figure 3) and the four unpaired electrons, i.e., CAS(4,4). Taking the minimal CAS, the energy gap between singlet and triplet states in **1** and **2** complexes has been computed to be -7.00 and -272 cm^{-1}, respectively. The huge increase ($J_{Pd}/J_{Ni} \approx 39$) of the antiferromagnetic coupling strength in **2** with respect to **1** is ascribed to the increase of the size of the interacting orbitals.[3l] Adding the dynamical correlation to the CASSCF wave functions, CASPT2 results augments these energy differences up to -48.6 and -999 cm^{-1} in **1** and **2**, respectively. The increase in **1** is somewhat more significant than in **2**.

The occupation numbers computed for σ- and δ-like active orbitals, shown in Table 2, present important differences. The former are considerably different from 1.00, indicating their strong engagement in magnetic interactions. Oppositely, δ orbitals do not participate so actively in the magnetism. This fact gets especially significant in the Pd complex, implying the existence of a very strong coupling between σ electrons such that some covalent bond is generated in the metal−metal region.

The J parameters obtained at the CASPT2 level with minimal CAS, despite being qualitatively correct, are typically far from being accurate (Table 3). For compound **1** the CASPT2 value of J is about 50% of the experimental value with a minimal CAS. This means that the inactive electrons and inactive orbitals

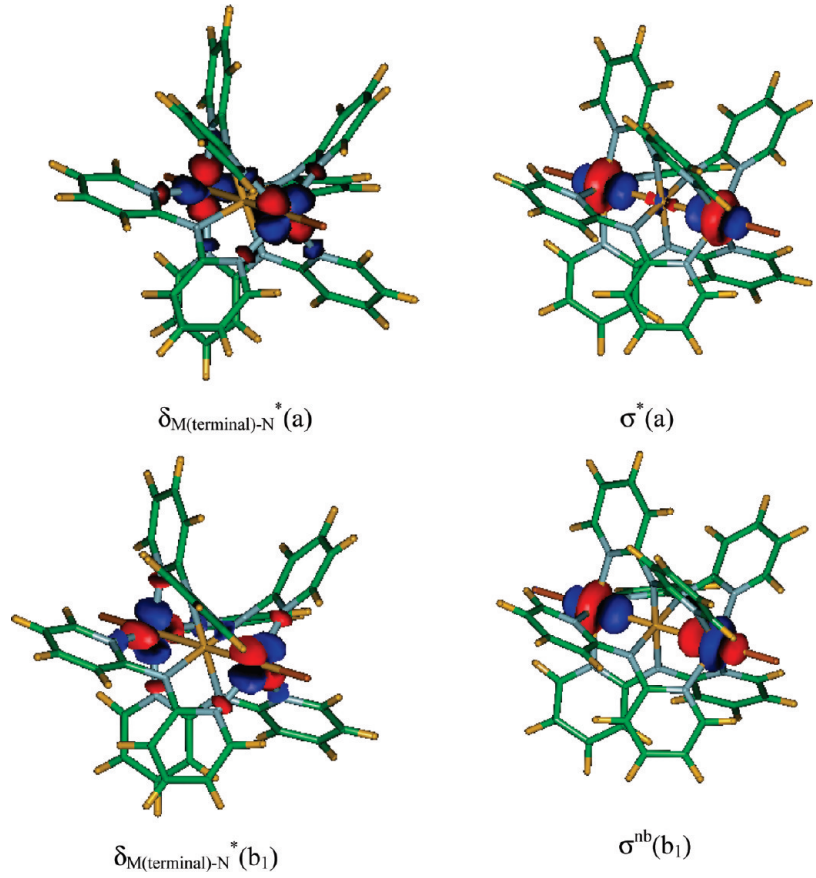

Figure 3. Magnetic orbitals involved in CAS(4,4) in **1** and **2**. The symmetry of each orbital is given in parentheses.

TABLE 2: Occupation Numbers of Active Orbitals in the CAS(4,4) in the Singlet Ground State for Compounds 1 and 2

compound	$\delta_{M(terminal)-N}$*(a)	$\delta_{M(terminal)-N}$*(b_1)	$\sigma^{nb}(b_1)$	σ*(a)
1	1.0006	0.9994	1.0219	0.9781
2	1.0032	0.9968	1.1789	0.8211

TABLE 3: Calculated $-J$ (in cm^{-1}) for Minimal and Extended Spaces at CASSCF and CASPT2 Levels for Compounds 1 and 2

compound	CAS(4,4)	CASPT2	CAS(10,13)	CASPT2	DFT[a]	exp.[d]
1	7.00	48.6	31.1	97.5	91[b]	99−108
2	272	999	612	1435	1393[c]	−

[a] B3LYP functional. [b] Ref 5c. [c] Ref 3l. [d] Refs 3a and 4a.

actually play a role in the accurate evaluation of the energy difference. It is not easy, though, to rationally enlarge the CAS. Also, its dimension may become prohibitive before giving an accurate value of the magnetic exchange. Which orbitals are actually the most important in the present magnetic problem? Knowing that the coupling mechanism between terminal metals occurs via the central metal in both pathways, we extend the active space with those orbitals that are mainly localized on the central metal. This central metal can be considered to play the role of the diamagnetic bridge in the standard Anderson superexchange model.[19] Including three doubly occupied orbitals, $\delta_{Ni(central)-N}$, σ, and $\delta_{Ni(central)}$ (see Figure 4a) produce large fluctuations in the occupation numbers (1.9671, 1.9471, and 1.9781, respectively) in the case of compound **1**. By including also their corresponding virtual orbitals, the CAS(10,13), as shown in Figure S1 in the Supporting Information, augments the magnitude of the antiferromagnetic interaction up to -31.1 cm^{-1} at the CASSCF level. For a complete quantitative agreement with experiment, we included the dynamic effects to the reference wave function. Hence, for **1** we obtained $J = -97.5$ cm^{-1}, in excellent agreement with experiments.

To see the effect of distance between magnetic centers upon J, the same calculations have been performed using the geometry of the molecule optimized in the quintet state with terminal Ni−Ni distances stretched to 4.976 Å (the previous Ni_{term}−Ni_{term} distance was 4.962 Å, corresponding to the ground state). The magnitude of J at the new distance is computed to be -91.7 cm^{-1}, smaller than the ground state one, -97.5 cm^{-1}. We observe that a tiny enlargement in the Ni−Ni distance causes a considerable decrease in J suggesting that the σ interaction, which takes place directly through the Ni−Ni axis, dominates the overall magnetic interaction. If we now perform these calculations with shorter Ni_{term}−Ni_{term} distances, like the experimental one (4.86 Å), a magnetostructural correlation can be obtained (see Figure 5). At this distance, J has been obtained as -168.3 cm^{-1}.[20] This large discrepancy with respect to experimental J raises the question of the performance of CASPT2 on systems with magnetic coupling arising from a dominating direct metal−metal σ interaction. The lack of information on this kind of systems does not help rationalize this behavior. The deformation of Ni−N bonds in the range of terminal Ni−Ni distances studied (ca. 0.1 Å) is negligible, and no effect upon J can be expected, especially because the dominating part of J comes from the σ Ni−Ni interaction.

Figure 4b displays the doubly occupied orbitals added to the minimal active space in complex **2**. We observe that the active orbitals are not exactly equivalent to those of the extended CAS for **1**. The $4p_z$ orbital of the central Pd automatically enters rather than the $\delta_{Pd(central)}$ of b_1 symmetry. This confirms that the σ magnetic interaction, which takes place along the z-axis, is

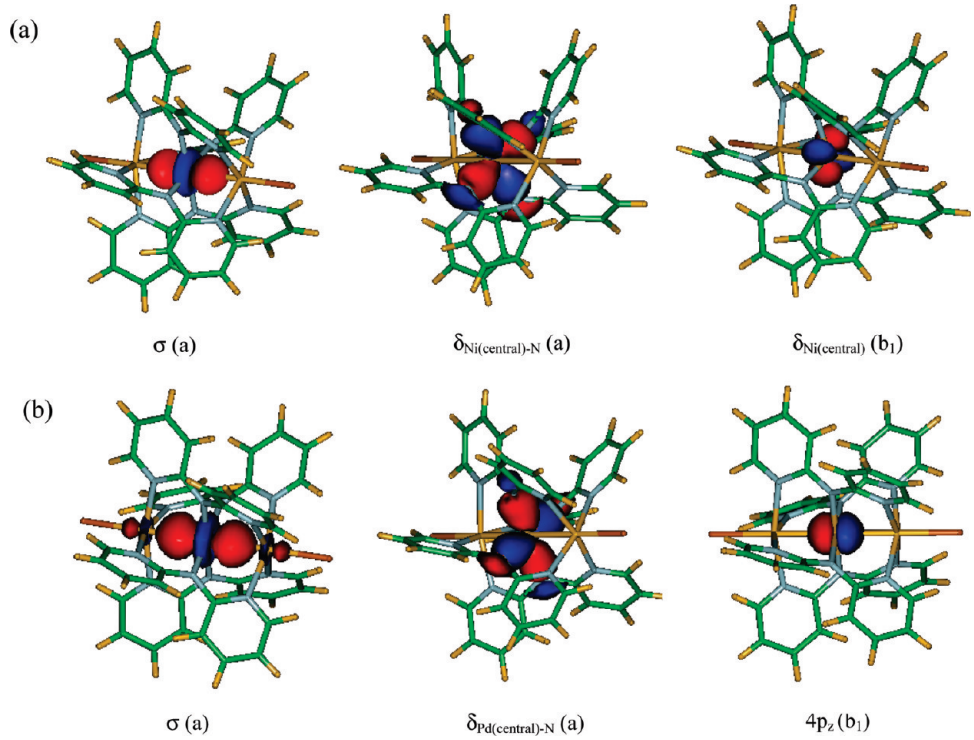

Figure 4. Doubly occupied orbitals added to the minimal CAS in (a) Ni and (b) Pd complexes. The symmetry of each orbital is given in parentheses.

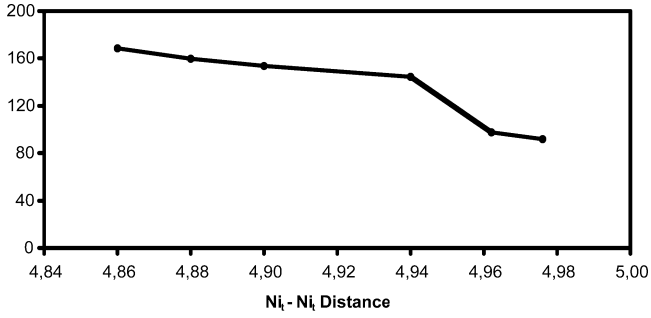

Figure 5. Value of magnetic coupling, $-J$ (cm^{-1}), as a function of the distance between the two terminal nickel atoms (Å).

stronger in **2** than in **1** (Table 3). Extending the active space (Figure S2, Supporting Information) in **2** mainly affects the CASSCF result. One may conclude that, in **2**, a minimal CAS can quantitatively describe the magnetic interaction since it fully contains the magnetic region. In other words, given that the magnetic orbitals localized on terminal Pd atoms are very voluminous (and the σ interaction is the dominant one), the role of the central metal orbitals is not so crucial, and a minimal CAS reproduces the major part of the magnetic coupling. The occupation numbers of $\delta_{Pd(central)-N}(a)$, $\sigma(a)$, and $4p_z(b_1)$ orbitals (1.9722, 1.9649, and 1.9976, respectively) show smaller fluctuations with respect to the same analysis made on the Ni complex. Here we report a magnitude of $J = -1435$ cm^{-1} for the exchange parameter in **2** which is of the same order as obtained by López et al. using DFT.[3l]

[Cu$_3$(dpa)$_4$Cl$_2$]$^+$ (3$^+$) and [Ag$_3$(dpa)$_4$Cl$_2$]$^+$ (4$^+$). In compounds $\mathbf{3}^+$ and $\mathbf{4}^+$, the magnetic coupling takes place between two unpaired electrons localized on the terminal atoms as in compounds **1** and **2** (Figure 2). However, the magnetic interaction takes place via δ-like orbitals, while the σ orbitals are inactive, doubly occupied orbitals. The unpaired electrons in the δ-system interact by a superexchange pathway involving the dpa ligands and the central metal ion, as demonstrated with

TABLE 4: Calculated $-J$ (cm^{-1}) for Minimal and Extended Spaces at CASSCF and CASPT2 Levels for the Cationic Species 3^+ and 4^+

compound	CAS(2,2)	CASPT2	extended CAS	CASPT2	DFT[a]	exp.[b]
$\mathbf{3}^+$	0.12	8.3	9.1[c]	34.8	64	34
$\mathbf{4}^+$	1.8	9.1	6.7[d]	138	265	–

[a] B3LYP functional, ref 3g. [b] Ref 3d. [c] CAS(14,13). [d] CAS(14,15).

DFT calculations.[3g] Considering the two singly occupied $\delta_{M(terminal)-N}$* orbitals, we get a minimal CAS(2,2). The exchange parameter computed for $\mathbf{3}^+$ is close to zero (Table 4). It has been demonstrated that the central metal, despite being diamagnetic, plays a key role in the superexchange coupling, lying at the crossing point of the magnetic interaction pathways.[3g] So, for a better performance of the calculations, an extended CAS must contain δ-type orbitals of the central copper. Nevertheless, extending the CAS with only these δ-type orbitals does not lead to a stable situation. The combined orbital and CI optimization process leads to a lower energy when the δ-functions on the central metal atom are changed to σ-type orbitals of this metal. Then, the tentative quest for increasing the number of magnetic electrons leads to adding six doubly occupied orbitals, i.e., $\delta_{M(terminal)}(a)$, $\delta_{M(central)-N}(a)$, σ*(a), $\delta_{N(terminal)-M}(b_1)$, $\delta_{M(terminal)}(b_1)$, and $\sigma^{nb}(b_1)$ (Figure 6 and Supporting Information, Figure S3), and their corresponding virtual orbitals to form a CAS(14,13). The magnitude of J significantly increases with this new active space. Among the added orbitals, the appearance of an orbital with mainly ligand character, $\delta_{N(terminal)-M}(b_1)$, is of interest since removal of this orbital leads to disordered states and makes the calculations fail. The presence of doubly occupied M(central)−N and virtual M(central)−N* orbitals in the active space emphasizes the importance of the central metal atom in the coupling. As a matter of fact, the considerable fluctuation observed in the occupation number of the metallic virtual orbital (0.160) might be evidence of this conclusion. Other theoretical works focused on these systems

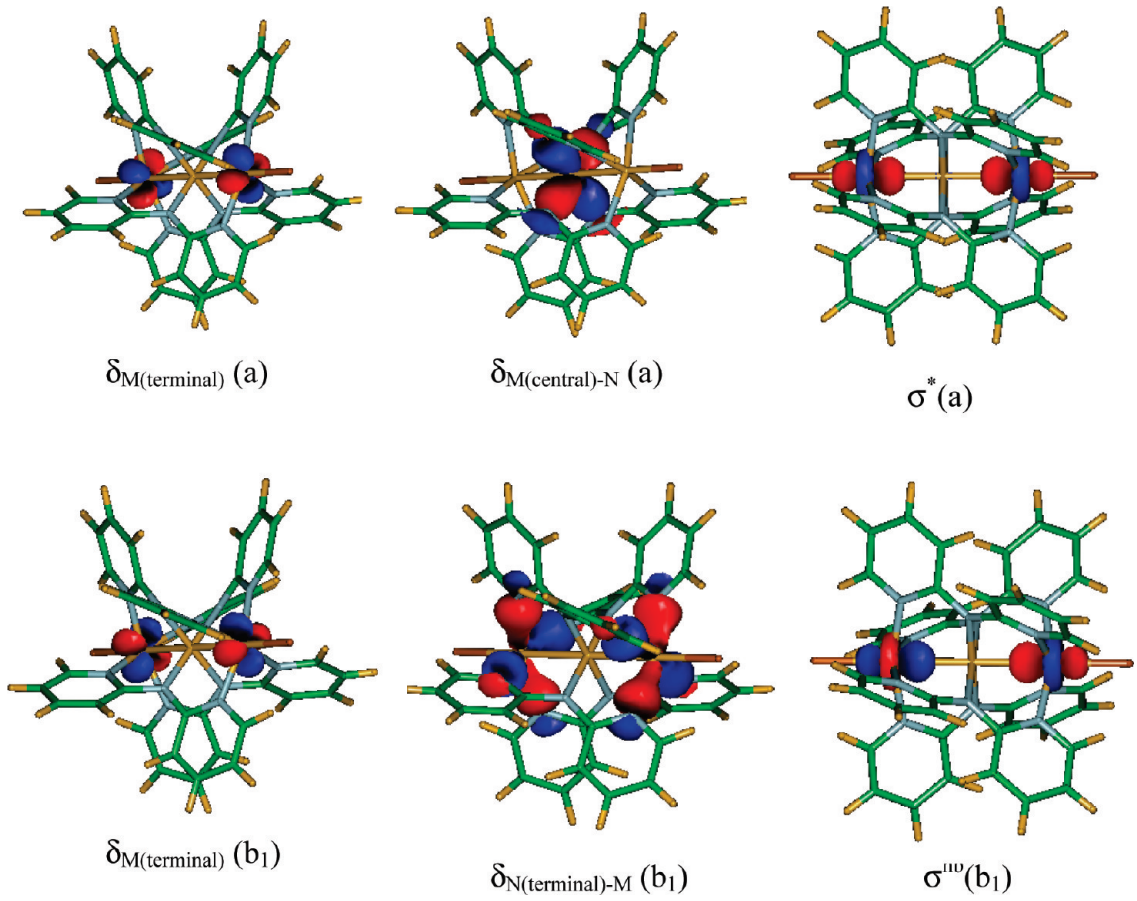

Figure 6. Doubly occupied orbitals added to the CAS(2,2) in $\mathbf{3}^+$ and $\mathbf{4}^+$. The symmetry of each orbital is given in parentheses.

have shown that the central metal atom plays a fundamental role in the magnetic coupling.[3g] Eventually, taking into account the dynamic correlation energy, $J = -34.8$ cm^{-1} for $\mathbf{3}^+$, in full agreement with the experimental value of -34 cm^{-1}. The present calculations solve the overestimation by a factor of 2 obtained by DFT method.

The strength of magnetic coupling in the hypothetical monocationic silver complex, $\mathbf{4}^+$, is expected to be larger than in $\mathbf{3}^+$, as DFT has predicted. This statement is based on the better overlap of x^2-y^2 orbitals of terminal silvers with the ligand orbitals. The triplet−singlet splitting energy obtained with a minimal CAS calculation is small but is already 1 order of magnitude larger than in $\mathbf{3}^+$, as shown in Table 4. Guided by the calculations on $\mathbf{3}^+$, we extend the CAS with both σ and δ orbitals as before to obtain a CAS(14,15) wave function. The corresponding J-value is more than 3.5 times larger than for the minimal CAS. Finally, $J = -138$ cm^{-1} at the CASPT2 level. The occupation numbers of the formally doubly occupied $\delta_{M(central)-N}$ and virtual $\delta_{M(central)-N}$* orbitals included in the extended CAS are larger/smaller than in $\mathbf{3}^+$ but still significantly far from 2 and 0 (1.938 and 0.063, respectively). The DFT calculated value of J is again two times larger than the present CASPT2 result.

The role of the dynamical correlation becomes evident when we compare the J-values of $\mathbf{3}^+$ and $\mathbf{4}^+$ at the different stages of the calculation. The coupling calculated with a CAS(2,2)SCF wave function is extremely small for both molecules. CASPT2 enhances the coupling in a similar fashion. The enlargement of the active space up to a CAS(14,15) leads to a modest increase of the coupling at the CASSCF level, but the inclusion of the dynamical electron correlation makes the difference: J increased by a factor of 4 in $\mathbf{3}^+$, while the increase is much more pronounced in $\mathbf{4}^+$. We stress that, in the final CASPT2 result for this latter molecule, no indications were found for intruder states. Reference weights do not differ by more than 0.001, and no configurations external to the CAS were found with small expectation values of H^0 or large interaction matrix elements.

2. Molecules with Three Magnetic Centers. *$Cu_3(dpa)_4Cl_2$* (3) *and* *$Ag_3(dpa)_4Cl_2$* (4). The $(M_3)^{6+}$ (M = Cu or Ag) backbone of the neutral complexes **3** and **4** contains three unpaired electrons, one more than the cationic $\mathbf{3}^+$ and $\mathbf{4}^+$ species. The extra electron in **3** and **4** is formally localized on the central metal atom, therefore becoming three-magnetic-center strings with $S = 1/2$ each. The highest δ orbitals, i.e., two $\delta_{Ni(terminal)-N}$* and one $\delta_{Ni(central)-N}$*, are singly occupied (see Figure 2). The three unpaired electrons are magnetically coupled. The magnetic exchange parameter in **3** and **4** originates, as in $\mathbf{3}^+$ and $\mathbf{4}^+$, from the interaction of δ-like magnetic electrons via the bridging dpa ligands. As mentioned above, the nearest-neighbor and next-nearest-neighbor interactions (J_1 and J_2, respectively) can be obtained from the eigenvalues of the spin Hamiltonian. In all hereafter calculations, $J_1 = J$ represents by far the strongest interaction, although the next-nearest neighbors parameter, J_2, is not always negligible (see the case of **4** in Table 5). The spectrum obtained by considering J_1 only or both J_1 and J_2 remains practically unchanged in **3**, but it is slightly different in **4**. However, neglecting J_2 does not change the general magnetism of these systems, and for the purpose of the present work, we just focus on the largest contribution, J_1.[21]

A primary description of the antiferromagnetic interaction between metal atoms at the CASSCF level can be given by choosing the three singly occupied δ orbitals (shown in Figure

TABLE 5: Calculated $-J$ (cm^{-1}) for the Minimal and Extended Spaces at CASSCF and CASPT2 Levels for the Neutral Species 3 and 4

compound	CAS(3,3)	CASPT2	extended CAS	CASPT2	DFT[a]	exp.[b]
3	9.8	53	33[c]	$J_1 = 122$ ($J_2 = 4.8$)	436	373
4	91	435	130[d]	$J_1 = 521$ ($J_2 = -37.6$)	1270	–

[a] B3LYP functional, ref 3g. [b] Ref 3c. [c] CAS(13,14). [d] CAS(13,13).

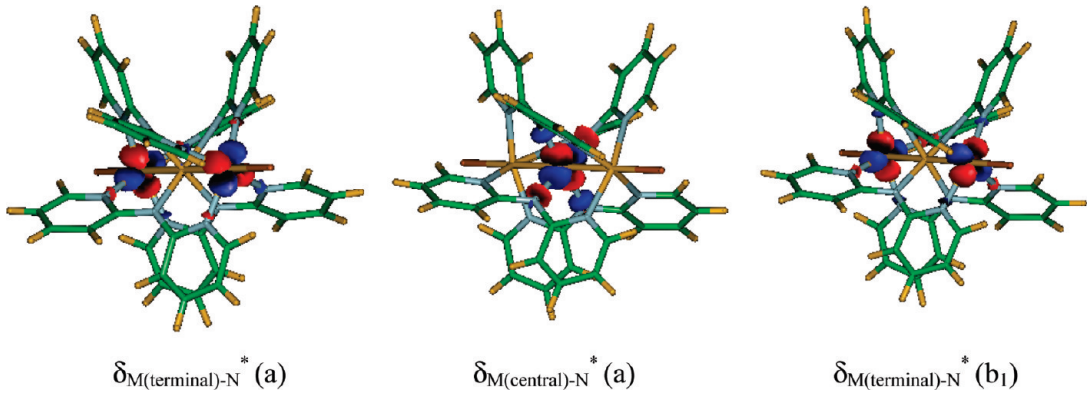

Figure 7. Orbitals involved in the CAS(3,3) in **3** and **4**. The symmetry of each orbital is given in parentheses.

7), as active orbitals: CAS(3,3). The calculations give $J = -9.8$ and -90.7 cm^{-1} for **3** and **4**, respectively (Table 5). The replacement of copper by silver in $M_3(dpa)_4Cl_2$ induces a tremendous increase of the coupling. More effective overlap between δ orbitals of Ag atoms and p atomic orbitals of nitrogen atoms is due to this increase. This trend is reproduced in CASPT2 calculations.

We tried to enlarge the active space with δ-type orbitals only, that is, with $\delta_{Cu(central)-N}(a)$ and $\delta_{Cu(terminal)}(a, b_1)$, but we faced problems similar to those in the cationic species mentioned before. In all the states, σ-type orbitals enter inevitably the active space, although they are not directly involved in magnetic interactions. Hence, the enlargement of the active space in **3** is carried out by entering the five doubly occupied orbitals, $\sigma(a)$, $\sigma^{nb}(b_1)$, $\delta_{Cu(central)-N}(a)$, $\sigma^*(a)$, and $\delta_{Cu(terminal)}(a)$, and their corresponding virtual orbitals to obtain a CAS(13,14), as shown in Figure 8 and Figure S5 (Supporting Information). The same orbitals were used to construct the extended CAS for compound **4** (Figure S6, Supporting Information). The only difference is that the $\delta_{Ag(terminal)}$ orbital has b_1 symmetry. The expansion of the active space enhances J at the CASSCF level up to -33 and -130 cm^{-1} for **3** and **4**, respectively. The increase of J is thus more important in the Cu_3 complex.

The value of J at the CASPT2 level reaches -122 cm^{-1} for **3**, which is about a factor of 3 smaller than the experimental value of -373 cm^{-1}. This is a rather unexpected result. Experience shows that CASPT2 based on a minimal CAS reproduces 50−70% of the experimental coupling, and after extending the active space even better agreement is usually obtained. Therefore, we explored possible sources for this notable discrepancy. The δ interaction occurs between adjacent metal atoms through some ligand bonds. Hence, not considering the ligand orbitals explicitly could be important in the superexchange mechanism influencing the final result. Accordingly, we intended to put additional ligand orbitals to the active space. Nevertheless, these ligand orbitals are transformed to Cu-d orbitals with extra radial nodes (so-called 3d′ orbitals) during the orbital optimization. These d orbitals significantly lower the total CASSCF energy but have no differential effect on the electronic states involved in the magnetic coupling process. The importance of introducing the ligand orbitals in the active space can be assessed by performing RASSCF calculations in which all ten Cu-3d orbitals are in the active space and additional configurations that involve single and double replacements in the occupied ligand orbitals and virtual Cu-3d′ orbitals are added to the wave function. Dynamical electron correlation can be introduced by means of the recently presented RASPT2 method.[22] This choice of active space gives the desired orbitals but does not affect the magnetic coupling parameter, $J = -92$ cm^{-1} for RASPT2, the same order of magnitude as our final CASPT2 estimate.

Similar conclusions have been derived from DDCI calculations on **3**. The full DDCI calculation is far too large to be completed, but the configuration space can be reduced by performing a dedicated orbital transformation on the molecular orbitals,[23] which orders the orbitals by increasing importance to the energy difference of the states of interest. After removing the less important orbitals, a DDCI calculation can be performed on **3**, resulting in an approximate $J = -75$ cm^{-1}, depending on the number of molecular orbitals considered in the calculation. The full DDCI value would probably be somewhat higher, but other DDCI calculations with dedicated molecular orbitals show that a reasonable estimate of J can be obtained with approximately 50% of the molecular orbitals,[23] exactly the range where the DDCI calculations for **3** have been performed. At present, we lack information to rationalize the anomalous large discrepancy between CASPT2 and experiment. Neither the perturbative approach nor the choice of active space can be the origin.

To rationalize the size of the coupling between the nearest neighbor Cu ions, we compare the EMAC system to the well-known benchmark molecule $Cu_2(ac)_4$ (ac = acetate), which shows a magnetic coupling constant of ~ -300 cm^{-1}, similar to what has been reported for **3**. The magnetic interaction path is similar for $Cu_2(ac)_4$ and **3**, but two important differences can be observed. In the first place, the Cu atoms in $Cu_2(ac)_4$ are coordinated by more electronegative atoms than in **3**, and second, the dihedral angle L−Cu−Cu−L (the twist angle) is zero in the acetate compound while it is as large as 21° in **3**. Small twist angles tend to increase the magnetic coupling as the direct exchange integral (ferromagnetic in nature) is reduced. However, for larger twist angles the magnetic interaction path

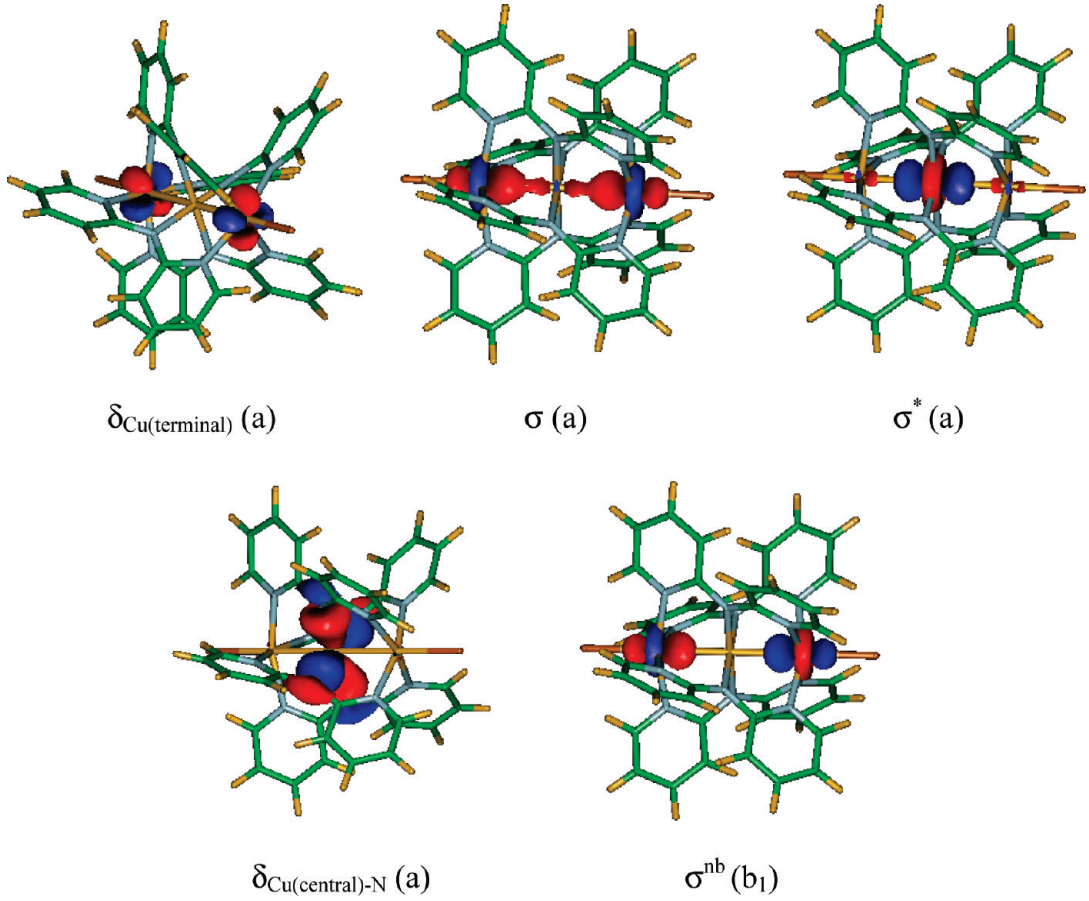

Figure 8. Doubly occupied orbitals added to CAS(3,3) in **3** and **4** complexes. The symmetry of each orbital is given in parentheses.

over the ligand becomes more distorted and less favorable, causing a reduction of the magnetic coupling constant. We have reduced the mentioned dihedral angle from an initial value of 21.3° to 16.3° and then to 13.3°. For smaller angles, the two hydrogens of neighboring pyridine rings become too close, and bonding interactions appear. The quantities of J for the two new dihedral angles have been calculated as -69 and -78 cm^{-1}, respectively, at the minimal CASPT2 level, which suffices for this qualitative analysis. The initial one was -53 cm^{-1}. This confirms that the large dihedral angle makes the coupling weaker. On the other hand, the weaker electronegativity of the N atoms coordinating the Cu ions in **3** favors a stronger coupling in comparison to $Cu_2(ac)_4$, where the first coordination sphere is formed by oxygens. The net effect of these opposite effects is difficult to estimate, but it seems reasonable that the magnetic coupling between nearest neighbors in **3** is approximately the same as in $Cu_2(ac)_4$. The slightly smaller Cu−Cu distance in **3** (2.53 vs 2.61 Å in $Cu_2(ac)_4$) can increase the importance of the direct exchange somewhat, but not to such an extent that the magnetic coupling is much smaller than in $Cu_2(ac)_4$ as predicted by our calculations.

For complex **4**, we report $J = -521$ cm^{-1}, which is less than half of the DFT value. The increase of magnitude of J in CASPT2 calculations in both complexes is similar, so the $J_{Ag}/J_{Cu} \approx 4$ ratio remains the same as for the extended CAS. In **4**, the effect of extending the CAS is not so considerable in CASPT2 calculations, and the J values of CASPT2 of minimal and extended CAS are similar.

Conclusions

The magnetic coupling parameter in a series of relatively large molecules (89 atoms) containing three TM atoms has been calculated with the CASSCF/CASPT2 method. Three groups of $M_3(dpa)_4Cl_2$ complexes have been studied in this work, with one real and one hypothetical molecule in each group. To facilitate the comparison of the results between real and hypothetic molecules, we used the same set of active orbitals for both cases. The most relevant conclusions are the following.

The calculated magnetic coupling constants J for real systems containing two magnetic centers (**1** and **3**$^+$) are in excellent agreement with the experimental values. On the other hand, calculations performed for **3**, a system with three magnetic centers, only provide ∼33% of the experimental J. Knowing that neither the perturbative approach nor the choice of active space can be the origin of such an anomalous large discrepancy between computed and experiment J, it might be interesting in the near future to look closer into the source of error. In hypothetical systems **2**, **4**, and **4**$^+$, the predictions made upon J are always smaller than those made by DFT. This behavior was expected beforehand. Compared to **1**, **3**, and **3**$^+$, respectively, the J values make sense at a qualitative level (as has been reported based on DFT) in relation to the spatial extent of the magnetic orbitals on the metal.

An important variation in the strength of J is found in $Ni_3(dpa)_4Cl_2$ when the distance between magnetic centers changes. This strong dependence of J on the metal−metal distance brings the conclusion that the interaction existing inline with the Ni_3 axis is the dominant part of the total magnetic coupling. That is, the magnetic interaction that occurs by means of the σ orbitals is much stronger than that coming from the δ orbitals. This particular issue is being explored in depth to get quantitative information.

Since the minimal CAS is not sufficient to obtain quantitatively correct J values, extended active spaces have been used

for all the complexes. These calculations reveal that the magnitude of J is very sensitive to the type and number of active orbitals. Indeed, a broad range of J-values is obtained as different orbitals are considered, especially in complexes in which J originates in δ interactions only, namely, **3**, **4**, $\mathbf{3}^+$, and $\mathbf{4}^+$. In contrast, the tentative determination of the most important orbitals in compounds of the $S = 1$ family, namely, **1** and **2**, is straightforward. As the magnetic interactions in the latter complexes are governed by σ and δ orbitals, selecting the orbitals necessary to obtain quantitatively correct J is undeviating and just needs to describe properly the σ part. This fact, although not proved here, may imply that the part of J coming from the coupling of electrons occupying σ orbitals is much stronger that that coming from δ electrons.

Despite the fact that the J parameters of **3**, **4**, $\mathbf{3}^+$, and $\mathbf{4}^+$ are attributed to a mechanism based on δ-like interactions, the existence of σ orbitals in an extended CAS is important to obtain quantitatively correct parameters. In other words, these calculations do not provide precise J parameters if just δ orbitals are included in the CAS. The exact character of the active orbitals in these extended CAS calculations is the result of a delicate balance between effects that mainly affect the magnetic interaction and other correlation effects that lower the total energy but do not contribute to the energy difference between the states of interest. In some cases, it may not be possible to introduce the desired orbitals in the CAS. Then the RASSCF approach may be an interesting option.

The CASPT2 method is an alternative to DFT in the calculation of magnetic parameters in large systems such as EMACs, giving results with semiquantitative precision. In all molecules discussed here, the dynamical electron correlation provides the main part of J.

Acknowledgment. Financial support has been provided by the Spanish Ministry of Science and Innovation (Project CTQ2008-06644-C02-01) and the Generalitat de Catalunya (Project 2009SGR462 and Xarxa de Referència en Química Teòrica i Computacional). X.L. thanks the Ramón y Cajal program (RYC-2008-02493).

Supporting Information Available: 3D views of the molecular orbitals included in the extended active spaces for all molecules. This material is available free of charge via the Internet at http://pubs.acs.org.

References and Notes

(1) (a) Itoh, K. Kinoshita, M., *Molecular Magnetism, New Magnetic Materials*, Gordon and Breach Science Pub.: Tokyo, 2000. (b) *Magnetism: Molecules to Materials*; Miller, J. S., Drillon, M., Eds.; Wiley-VCH, 2001.

(2) (a) Chien, C. H.; Chang, J. C.; Yeh, C. Y.; Lee, G. H.; Fang, J. M.; Peng, S. M. *J. Chem. Soc., Dalton Trans.* **2006**, 2106. (b) Bera, J. K.; Dunbar, K. R. *Angew. Chem., Int. Ed.* **2002**, *41*, 4453. (c) Pyrka, G. J.; El-Mekki, M.; Pinkerton, A. A. *J. Chem. Soc., Chem. Commun.* **1991**, 84. (d) Tejel, C.; Ciriano, M. A.; Villarroya, B. E.; Gelpi, R.; López, J. A.; Lahoz, F. J.; Oro, L. A. *Angew. Chem., Int. Ed.* **2001**, *40*, 4084. (e) Robertson, N.; McGowan, C. A. *Chem. Soc. Rev.* **2003**, *32*, 96. (f) Carroll, R. L.; Gorman, C. B. *Angew. Chem., Int. Ed.* **2002**, *41*, 4378. (g) Murahashi, T.; Higuchi, Y.; Katoh, T.; Kurosawa, H. *J. Am. Chem. Soc.* **2002**, *124*, 14288. (h) Ruffer, T.; Ohashi, M.; Shima, A.; Mizomoto, H.; Kaneda, Y.; Mashima, K. *J. Am. Chem. Soc.* **2004**, *126*, 12244.

(3) (a) Clérac, R.; Cotton, F. A.; Dunbar, K. R.; Murillo, C. A.; Pascual, I.; Wang, X. *Inorg. Chem.* **1999**, *38*, 2655. (b) Berry, J. F.; Cotton, F. A.; Lu, T.; Murillo, C. A.; Roberts, B. K.; Wang, X. *J. Am. Chem. Soc.* **2004**, *126*, 7082. (c) Berry, J. F.; Cotton, F. A.; Peng, L.; Murillo, C. A. *Inorg. Chem.* **2003**, *42*, 377. (d) Berry, J. F.; Cotton, F. A.; Daniels, L. M.; Murillo, C. A.; Wang, X. *Inorg. Chem.* **2003**, *42*, 2418. (e) Rohmer, M. M.; Bénard, M. *J. Am. Chem. Soc.* **1998**, *120*, 9372. (f) Rohmer, M. M.; Strich, A.; Bénard, M.; Malrieu, J. P. *J. Am. Chem. Soc.* **2001**, *123*, 9126. (g) Bénard, M.; Berry, J. F.; Cotton, F. A.; Gaudin, C.; López, X.; Murillo, C. A.; Rohmer, M. M. *Inorg. Chem.* **2006**, *45*, 3932. (h) López, X.; Bénard, M.; Rohmer, M.-M. *THEOCHEM* **2006**, *777*, 53. (i) López, X.; Bénard M.; Rohmer, M. M. *Inorg. Chem.* **2007**, *46*, 5. (j) Rohmer, M.-M.; Liu, I. P.-C.; Lin, J.-C.; Chiu, M.-J.; Lee, C.-H.; Lee, G.-S.; Bénard, M.; López, X.; Peng, S.-M. *Angew. Chem., Int. Ed.* **2007**, *46*, 3533. (k) Liu, I. P.-C.; Lee, G. H.; Peng, S. M.; Bénard, M.; Rohmer, M. M. *Inorg. Chem.* **2007**, *46*, 9602. (l) López, X.; Rohmer, M. M.; Bénard, M. *J. Mol. Struct.* **2008**, *890*, 18. (m) Labeguerie, P.; Rohmer, M. M.; Bénard, M. *J. Chin. Chem. Soc.* **2009**, *56*, 22.

(4) (a) Peng, S. M.; Wang, C. C.; Jang, Y. L.; Chen, Y. H.; Li, F. Y.; Mou, C. Y.; Leung, M. K. *J. Magn. Magn. Mater.* **2000**, *209*, 80. (b) Hasan, H.; Tan, U. K.; Lee, G. H.; Peng, S. M. *Inorg. Chem. Commun.* **2007**, *10*, 983. (c) Tsao, T. B.; Lo, S. S.; Yeh, C. Y.; Lee, G. H.; Peng, S. M. *Polyhedron* **2007**, *26*, 3833. (d) Lai, S. Y.; Lin, T. W.; Chen, Y. H.; Wang, C. C.; Lee, G. H.; Yang, M. H.; Leung, M. K.; Peng, S. M. *J. Am. Chem. Soc.* **1999**, *21*, 250. (e) Cotton, F. A.; Daniels, L. M.; Lu, T.; Murillo, C. A.; Wang, X. *Chem. Commun.* **1999**, 2461. (f) Cotton, F. A.; Daniels, L. M.; Lu, T.; Murillo, C. A.; Wang, X. *J. Chem. Soc., Dalton Trans.* **1999**, 517. (g) Chang, H. C.; Li, J. T.; Wang, C. C.; Lin, T. W.; Lee, H. C.; Lee, G. H.; Peng, S. M. *Eur. J. Inorg. Chem.* **1999**, 1243. (h) Shieh, S. J.; Chou, C. C.; Lee, G. H.; Wang, C. C.; Peng, S. M. *Angew. Chem., Int. Ed. Engl.* **1997**, *36*, 56. (i) Yeh, C. Y.; Chou, C. H.; Pan, K. C.; Wang, C. C.; Lee, G. H.; Su, Y. O.; Peng, S. M. *J. Chem. Soc., Dalton Trans.* **2002**, 2670. (j) Wang, C. C.; Lo, W. C.; Chou, C. C.; Lee, G. H.; Chen, J. M.; Peng, S. M. *Inorg. Chem.* **1998**, *37*, 4059. (k) Yeh, C. Y.; Chiang, Y. L.; Lee, G. H.; Peng, S. M. *Inorg. Chem.* **2002**, *41*, 4096. (l) Chen, Y. H.; Lee, C. C.; Wang, C. C.; Lai, S. Y.; Li, F. Y.; Mou, C. Y.; Peng, S. M. *Chem. Commun.* **1999**, 1667. (m) Lai, S. Y.; Wang, C. C.; Chen, Y. H.; Lee, C. C.; Liu, Y. H.; Peng, S. M. *J. Chin. Chem. Soc.* **1999**, *46*, 477. (n) Liu, I. P. C.; Lee, G. H.; Peng, S. M.; Bénard, M.; Rohmer, M. M. *Inorg. Chem.* **2007**, *46*, 9602. (o) Liu, I. P. C.; Wang, W. Z.; Peng, S. M. *Chem. Commun.* **2009**, 4323. (p) Yin, C. X.; Su, J.; Huo, F. J.; Ismayilov, R. H.; Wang, W. Z.; Lee, G. H.; Yeh, C. Y.; Peng, S. M. *J. Coord. Chem.* **2009**, *62*, 2974. (q) Huang, G. C.; Liu, I. P. C.; Kuo, J. H.; Huang, Y. L.; Yeh, C. Y.; Lee, G. H.; Peng, S. M. *Dalton. Trans.* **2009**, 2623. (r) Rohmer, M. M.; Liu, I. P. C.; Lin, J. C.; Chiu, M. J.; Lee, C. H.; Lee, G. H.; Bénard, M.; López, X.; Peng, S. M. *Angew. Chem., Int. Ed.* **2007**, *46*, 3533. (s) Huang, G. C.; Bénard, M.; Rohmer, M. M.; Li, L. A.; Chiu, M. J.; Yeh, C. Y.; Lee, G. H.; Peng, S. M. *Eur. J. Inorg. Chem.* **2008**, 1767. (t) Lai, S. H.; Hsiao, C. J.; Ling, J. W.; Wang, W. Z.; Peng, S. M.; Chen, I. C. *Chem. Phys. Lett.* **2008**, *456*, 181. (u) Yin, C.; Huang, G. C.; Kuo, C. K.; Fu, M. D.; Lu, H. C.; Ke, J. H.; Shih, K. N.; Huang, Y. L.; Lee, G. H.; Yeh, C. Y.; Chen, C. H.; Peng, S. M. *J. Am. Chem. Soc.* **2008**, *130*, 10090.

(5) (a) Cotton, F. A.; Daniels, L. M.; Murillo, C. A.; Pascual, I. *J. Am. Chem. Soc.* **1997**, *119*, 10223. (b) Clérac, R.; Cotton, F. A.; Daniels, L. M.; Dunbar, K. R.; Murillo, C. A.; Pascual, I. *Inorg. Chem.* **2000**, *39*, 748. (c) Clérac, R.; Cotton, F. A.; Daniels, L. M.; Dunbar, K. R.; Murillo, C. A.; Pascual, I. *Inorg. Chem.* **2000**, *39*, 752. (d) Cotton, F. A.; Daniels, L. M.; Lei, P.; Murillo, C. A.; Wang, X. *Inorg. Chem.* **2001**, *40*, 2778. (e) Berry, J. F.; Cotton, F. A.; Murillo, C. A.; Roberts, B. K. *Inorg. Chem.* **2004**, *43*, 2277. (f) Cotton, F. A.; Chao, H.; Murillo, C. A.; Wang, Q. *Dalton Trans.* **2006**, 5416. (g) Berry, J. F.; Cotton, F. A.; Lei, P.; Lu, T.; Murillo, C. A. *Inorg. Chem.* **2003**, *42*, 3534. (h) Berry, J. F.; Cotton, F. A.; Fewox, C. S.; Lu, T.; Murillo, C. A. *Dalton Trans.* **2004**, 2297. (i) Berry, J. F.; Cotton, F. A.; Murillo, C. A. *Dalton Trans.* **2003**, 3015. (j) Berry, J. F.; Cotton, F. A.; Murillo, C. A. *Organometallics.* **2004**, *23*, 2503.

(6) (a) Berry, J. F.; Cotton, F. A.; Daniels, L. M.; Murillo, C. A. *J. Am. Chem. Soc.* **2002**, *124*, 3212. (b) Berry, J. F.; Cotton, F. A.; Lu, T.; Murillo, C. A.; Wang, X. *Inorg. Chem.* **2003**, *42*, 3595. (c) Kiehl, P.; Rohmer, M. M.; Bénard., M. *Inorg. Chem.* **2004**, *43*, 3151.

(7) (a) Andersson, K.; Malmqvist, P.-Å.; Roos, B. O.; Sadlej, A. J.; Wolinski, K. *J. Phys. Chem.* **1990**, *94*, 5483. (b) Andersson, K.; Malmqvist, P.-Å.; Roos, B. O. *J. Chem. Phys.* **1992**, *96*, 1218.

(8) Miralles, J.; Daudey, J.-P.; Caballol, R. *Chem. Phys. Lett.* **1992**, *198*, 555.

(9) (a) Beebe, N. H. F.; Linderberg, J. *Int. J. Quantum Chem.* **1997**, *7*, 683. (b) Koch, H.; Sánchez de Merás, A.; Pedersen, T. B. *J. Chem. Phys.* **2003**, *118*, 9481. (c) Aquilante, F.; Malmqvist, P.-Å.; Pedersen, T. B.; Ghosh, A.; Roos, B. O. *J. Chem. Theory. Comput.* **2008**, *4*, 694.

(10) Saebo, S.; Pulay, P. *Annu. Rev. Phys. Chem.* **1993**, *44*, 213. (b) Schütz, M.; Werner, H. J. *J. Chem. Phys.* **2001**, *114*, 661. (c) Subotnik, J. E.; Sodt, A.; Head-Gordon, M. *J. Chem. Phys.* **2008**, *128*, 034103. (d) Bessac, F.; Hoyau, S.; Maynau, D. *J. Chem. Phys.* **2005**, *123*, 104105.

(11) Ayed, T.; Guihéry, N.; Tangour, B.; Barthelat, J. C. *Theor. Chem. Acc.* **2006**, *116*, 497.

(12) (a) Andersson, K.; Malmqvist, P.-Å.; Roos, B. O.; Sadlej, A. J.; Wolinski, K. *J. Phys. Chem.* **1990**, *94*, 5483. (b) Andersson, K.; Malmqvist, P.-Å.; Roos, B. O. *J. Chem. Phys.* **1992**, *96*, 1218.

(13) (a) de Graaf, C.; Broer, R.; Nieuwpoort, W. C. *Chem. Phys. Lett.* **1997**, *271*, 372. (b) Yamanaka, S.; Okumura, M.; Nagao, H.; Yamaguchi, K. *Chem. Phys. Lett.* **1995**, *233*, 88. (c) de Graaf, C.; Illas, F. *Phys. Rev. B* **2001**, *63*, 014404. (d) Sousa, C.; de Graaf, C.; Illas, F.; Pacchioni, G. *Prog. Theor. Chem. Phys.* **2000**, *7*, 227. (e) de Graaf, C.; Sousa, C.; de P. R. Moreira, I.; Illas, F. *J. Phys. Chem. A* **2001**, *105*, 11371. (f) Ceulemans,

A.; Heylen, G. A.; Chiboatru, L. F.; Maes, T. L.; Pierloot, K.; Ribbing, C.; Vanquickenborne, L. G. *Inorg. Chim. Acta* **1996**, *251*, 15. (g) Hendrickx, M. F. A.; Clima, S.; Chibotaru, L.; Ceulemans, A. *J. Phys. Chem. A* **2005**, *109*, 8857.

(14) Frisch, M. J.; Trucks, G. W.; Schlegel, H. B.; Scuseria, G. E.; Robb, M. A.; Cheeseman, J. R.; Montgomery, J. A., Jr.; Vreven, T.; Kudin, K. N.; Burant, J. C.; Millam, J. M.; Iyengar, S. S.; Tomasi, J.; Barone, V.; Mennucci, B.; Cossi, M.; Scalmani, G.; Rega, N.; Petersson, G. A.; Nakatsuji, H.; Hada, M.; Ehara, M.; Toyota, K.; Fukuda, R.; Hasegawa, J.; Ishida, M.; Nakajima, T.; Honda, Y.; Kitao, O.; Nakai, H.; Klene, M.; Li, X.; Knox, J. E.; Hratchian, H. P.; Cross, J. B.; Bakken, V.; Adamo, C.; Jaramillo, J.; Gomperts, R.; Stratmann, R. E.; Yazyev, O.; Austin, A. J.; Cammi, R.; Pomelli, C.; Ochterski, J. W.; Ayala, P. Y.; Morokuma, K.; Voth, G. A.; Salvador, P.; Dannenberg, J. J.; Zakrzewski, V. G.; Dapprich, S.; Daniels, A. D.; Strain, M. C.; Farkas, O.; Malick, D. K.; Rabuck, A. D.; Raghavachari, K.; Foresman, J. B.; Ortiz, J. V.; Cui, Q.; Baboul, A. G.; Clifford, S.; Cioslowski, J.; Stefanov, B. B.; Liu, G.; Liashenko, A.; Piskorz, P.; Komaromi, I.; Martin, R. L.; Fox, D. J.; Keith, T.; Al-Laham, M. A.; Peng, C. Y.; Nanayakkara, A.; Challacombe, M.; Gill, P. M. W.; Johnson, B.; Chen, W.; Wong, M. W.; Gonzalez, C.; and Pople, J. A.; *Gaussian 03*, Revision C.01; Gaussian, Inc.: Wallingford, CT, 2003.

(15) Karlström, G.; Lindh, R.; Malmqvist, P.-Å.; Roos, B. O.; Ryde, U.; Veryazov, V.; Widmark, P.-O.; Cossi, M.; Schimmelpfennig, B.; Neograd y, P.; Seijo, L. *Comput. Mater. Sci.* **2003**, *28*, 222. MOLCAS Version 7.0. Department of Theoretical Chemistry, University of Lund.

(16) (a) Roos, B. O.; Lindh, R.; Malmqvist, P.- Å.; Veryazov, V.; Widmark, P.-O. *J. Phys. Chem. A.* **2005**, *109*, 6575. (b) Roos, B. O.; Lindh, R.; Malmqvist, P.-Å.; Veryazov, V.; Widmark, P.-O. *J. Phys. Chem. A* **2004**, *108*, 2851.

(17) (a) Dirac, P. A. M. *Proc. R. Soc. London, Ser. A* **1926**, *112*, 661; **1929**, *123*, 714. (b) Heisenberg, W. *Z. Phys.* **1926**, *38*, 411. (c) van Vleck, J. H. *Theory of electric and Magnetic Susceptibilities*; Oxford University Press: London, 1932.

(18) Queralt, N.; Taratiel, D.; de Graaf, C.; Caballol, R.; Cimiraglia, R.; Angeli, C. *J. Comput. Chem.* **2008**, *29*, 994.

(19) Anderson, P. W. *Phys. Rev.* **1959**, *115*, 2.

(20) The geometry of molecule **1** with experimental Ni−Ni distance has been obtained by keeping the Cl−Ni−Ni−Ni−Cl chain frozen and optimizing the rest of the molecule with DFT.

(21) We simulated the magnetic susceptibility curve (χT vs T) for the Cu_3 complex with $J_2 = 0$ and -4.8 cm^{-1} resulting in two perfectly superimposed curves up to 300 K.

(22) Malmqvist, P.-Å.; Pierloot, K.; Rehaman, A.; Shahi, M.; Cramer, C. J.; Gagliardi, L. *J. Chem. Phys.* **2008**, *128*, 204109.

(23) Calzado, C. J.; Malrieu, J.-P.; Cabrero, J.; Caballol, R. *J. Phys. Chem. A* **2000**, *104*, 11636.

JP910763D